Supporting information for:

Ca^{2+} accelerates peptide fibrillogenesis via a heterogeneous secondary nucleation pathway

Kuo Zhang[1,2], Yong-Hong Gao[1,2], Wei-Shen Zhong[3], Hui Cao[1,*], Kai Yue[3,*], Lei Wang[2,*], and Hao Wang[2]

1 State Key Laboratory for Advanced Metals and Materials, School of Materials Science and Engineering, University of Science and Technology Beijing, Beijing 100083, China

2 CAS Center for Excellence in Nanoscience, CAS Key Laboratory for Biomedical Effects of Nanomaterials and Nanosafety, National Center for Nanoscience and Technology (NCNST), No. 11 Beiyitiao, Zhongguancun, Beijing, 100190, China

3 School of Energy and Environmental Engineering, University of Science and Technology Beijing, No. 30 Xueyuan Road, Beijing, 100083, China

Equations:

$$\lg[-\ln(1-X_{(t)})] = n\lg t + \lg K \quad (1)$$

Materials and Methods

Materials LAFH was purchased from GL Biochem. DMSO and hexafluoroisopropanol were purchased from Aladdin. ThT was purchased from Yuanye. ANS was purchased from TCI. $CaCl_2$ and phosphotungstic acid were purchased from Beijing Chemical Industry. Deionized water for the preparation of solution was used as received without further purification.

Differential scanning calorimetry (DSC) The samples for DSC measurement were performed on a DSC 8500 (Perkin Elmer, U.S.A.). 10 μL of LAFH (4 mM in DMSO) was added into water (0.99 mL) and 10 μL of $CaCl_2$ solution (4 mM in H_2O) was added to the solution immediately. About 40 mg of the resultant solution was added into a stainless-steel crucible and sealed. The thermodynamic parameters were collected under temperature of 28 °C. The data were representation of 3 individual experiments.

Circular Dichroism (CD) The samples for CD measurement were performed on a J-1500 (Jacso, Japan). 8 μL of LAFH (10 mM in hexafluoroisopropanol) was added into water (2 mL) and 20 μL of $CaCl_2$ solution (4 mM in H_2O) was added to the solution immediately. The CD spectrum was collected under temperature of 28 °C. The data was representation of 3 individual experiments.

TEM The samples for TEM observation were performed on a HT-7700 TEM (HITACHI, Japan). 10 μL of LAFH (4 mM in DMSO) was added into water (0.99 mL). 10 μL of $CaCl_2$ solution in different concentration (i.e. 4, 40, 400 mM in H_2O) was added to the solution immediately. The resultant solution was restored in oven with temperature

of 28°C. For the preparation of each sample, 10 μL of resultant solution was dropped on a copper mesh for 1 min and removed by filter paper. 10 μL of phosphotungstic acid (2% wt. in H_2O) was dropped as dye for 2 min and further removed by filter paper. The data was representation of 3 individual experiments.

Fluorescence intensity measurement of ANS/ThT The samples in solution for fluorescence intensity measurement were performed on a multi-mode microplate reader (Enspire, Perkin Elmer, U.S.A.). LAFH (4 mM in DMSO) was added into water to obtain LAFH in different concentrations. $CaCl_2$ solution in different concentration (i.e. 4, 40, 400 mM in H_2O) was added to the solution immediately followed by ANS/ThT (4 mM in DMSO). The fluorescence intensity was collected under temperature of 28°C with excitation wavelength of 375 nm and emission wavelength of 495 nm (ANS), excitation wavelength of 430 nm and emission wavelength of 490 nm (ThT) for every 3 min. The data was average of 6 individual samples.

Powder XRD The samples for XRD measurement were performed on Xeuss SAXS/WAXS system (Xenocs Asia Pacific Pte. Ltd. The LAFH was dissolved into hexafluoroisopropanol and dried by N_2. The resultant LAFH sample was recognized as amorphous state. For other samples, 50 μL of LAFH (4 mM in DMSO) was added into water (4.95 mL) and 50 μL of $CaCl_2$ solution (4 mM in H_2O) was added to the solution immediately. The resultant solution was restored in oven with temperature of 28 °C. The solution was fast freezing by liquid N_2 in specific time point (i.e. 0, 0.5, 1.5, 3 h) and further lyophilized to obtain powders for measurement.

Molecular Dynamics Simulation Periodic boundary conditions were adopted, the models of LAFH and integrin $\alpha_v\beta_3$ were generated by Automated Topology Builder (ATB). The X-ray structure of integrin $\alpha_v\beta_3$ was obtained from Protein Data Bank (PDB). Integrin $\alpha_v\beta_3$ protein downloaded from PDB Database (PDB ID: 4G1M) and gromos54a7 force field was selected. The NPT ensemble was used in the simulation process, which indicated that the atomic number, pressure and temperature of the system remained unchanged during the calculation process. The assembly of LAFH monomers without integrin $\alpha_v\beta$ was studied. The step size was 1 fs and the total simulation time was 120 ns. For the van der Waals interaction energy, the cutoff distance was set to 1.2 nm and the van der Waals force was represented by the Lennard-Jones potential. For the electrostatic interaction energy, the PME potential was used. The temperature of the system was maintained at 310 K by Berendsen hot bath. The pressure coupling mode was Berendsen and the pressure was 1 bar. Post-processing and visualization were implemented by software VMD, and all simulations were completed by Gromacs.

ThT fluorescence during LAFH fibrillogenesis without Ca^{2+}.

As shown in Figure S10a, there was almost no initial baseline, indicating that the primary nucleation occurred in a very short time. The fast rising of fluorescence intensity of ThT suggested fibrillogenesis of LAFH. The concentration dependent fibrillogenesis of LAFH monitored by ThT fluorescence experiments revealed that LAFH with higher concentration exhibited faster speed to accomplish fibrillogenesis (Figure S10a). ThT fluorescence data were fitted through AmyloFit, a useful tool to investigate the mechanism of fibrillogenesis on amyloid proteins.[1] The fitted curve based on secondary nucleation was the most consistent with the fluorescence data in all three concentrations, indicating the secondary nucleation mechanism of fibrillogenesis of LAFH without Ca^{2+} (Figure S10a).

The fluorescence intensity of ThT in LAFH with different concentrations was normalized, representing the ratio of fibrillogenesis, i.e. ($X_{(t)}$). As shown in Figure S10b, the dash lines fitted from measured data of $lg[-ln(1-X_{(t)})]$ versus lg t were not a single straight line in each concentration (equation S1), suggesting that fibrillogenesis of LAFH contained the process of secondary nucleation.[2]

ThT fluorescence during LAFH fibrillogenesis with Ca^{2+}.

The fibrillogenesis of LAFH (10, 20 and 40 μM) incubated with Ca^{2+} (40 μM) was further monitored through the fluorescence intensity of ThT. It was found that the fibrillogenesis was faster when the concentration of LAFH was increased (Figure S10c). The fitted curve of ThT fluorescence from AmyloFit also suggested that the fibrillogenesis of LAFH in different concentrations in the presence of Ca^{2+} was

secondary nucleation dominated process (Figure S10c). The dash lines fitted from ThT fluorescence data of different concentrations of LAFH with Ca^{2+} all consisted of two intersecting straight lines, confirming the occurrence of secondary nucleation in the fibrillogenesis of LAFH with Ca^{2+} (Figure S10d).

Comparison of ThT fluorescence and TEM during LAFH fibrillogenesis without/with Ca^{2+}.

For the high concentration of Ca^{2+}, TEM images validated the Ca^{2+} accelerated fibrillogenesis of LAFH, in which mountains of fibrous structure at 30 min (400 μM of Ca^{2+}, Figure S5) and 9 min (4000 μM of Ca^{2+}, Figure S6) with bundle-like NFs were observed, respectively. The fluorescence of ThT (40 μM) in LAFH with Ca^{2+} (400 or 4000 μM) was increased over time and the highest fluorescence intensities were much higher than that of LAFH with 0 and 40 μM Ca^{2+} groups (Figure S11). These results indicated that bundle-like NFs of LAFH with high concentration of Ca^{2+} may have large β-sheet structures, which can be recognized by ThT with high fluorescence. Higher concentration of Ca^{2+} of 4000 μM resulted in more bundled NFs of LAFH than concentration of Ca^{2+} of 400 μM, leading to higher fluorescence intensity of ThT.

The results suggested that ThT were not suitable for the precise measurement of β-sheet structures during fibrillogenesis of LAFH in low concentration of Ca^{2+}.

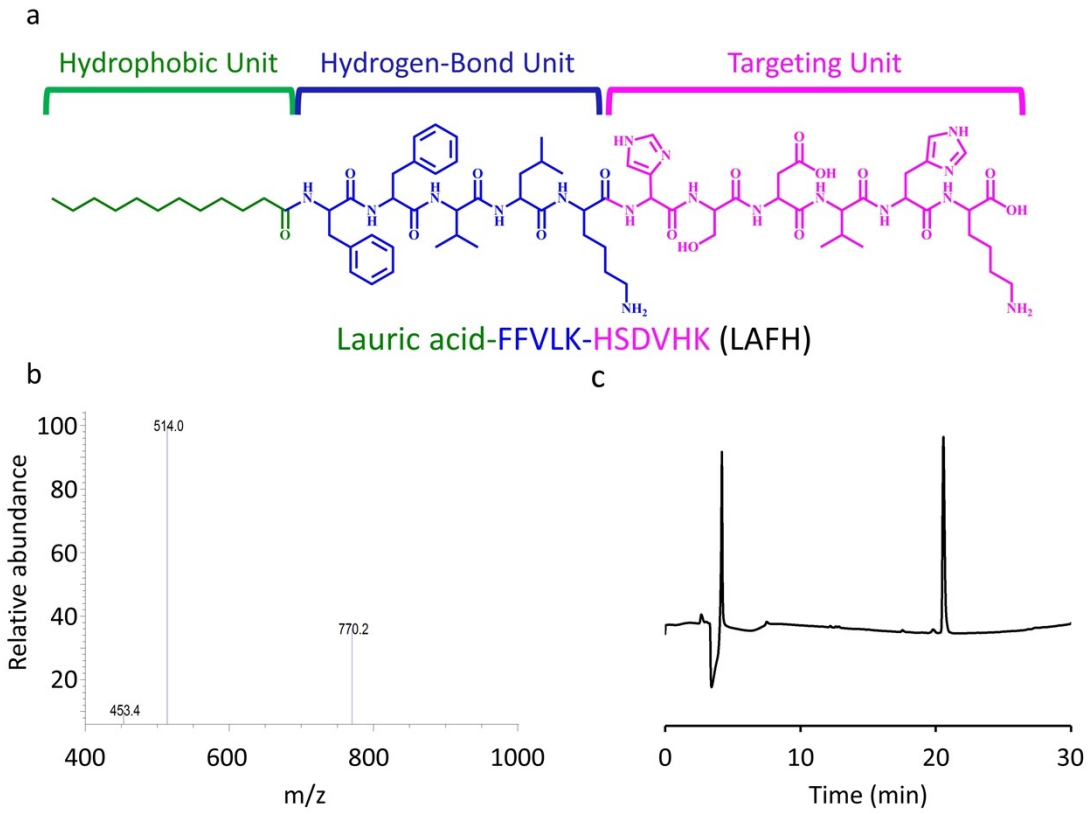

Figure S1. a) Molecular structure of LAFH. b,c) Electrospray Ionization Mass Spectra (b) and High Performance Liquid Chromatography (HPLC) spectra (c) of LAFH.

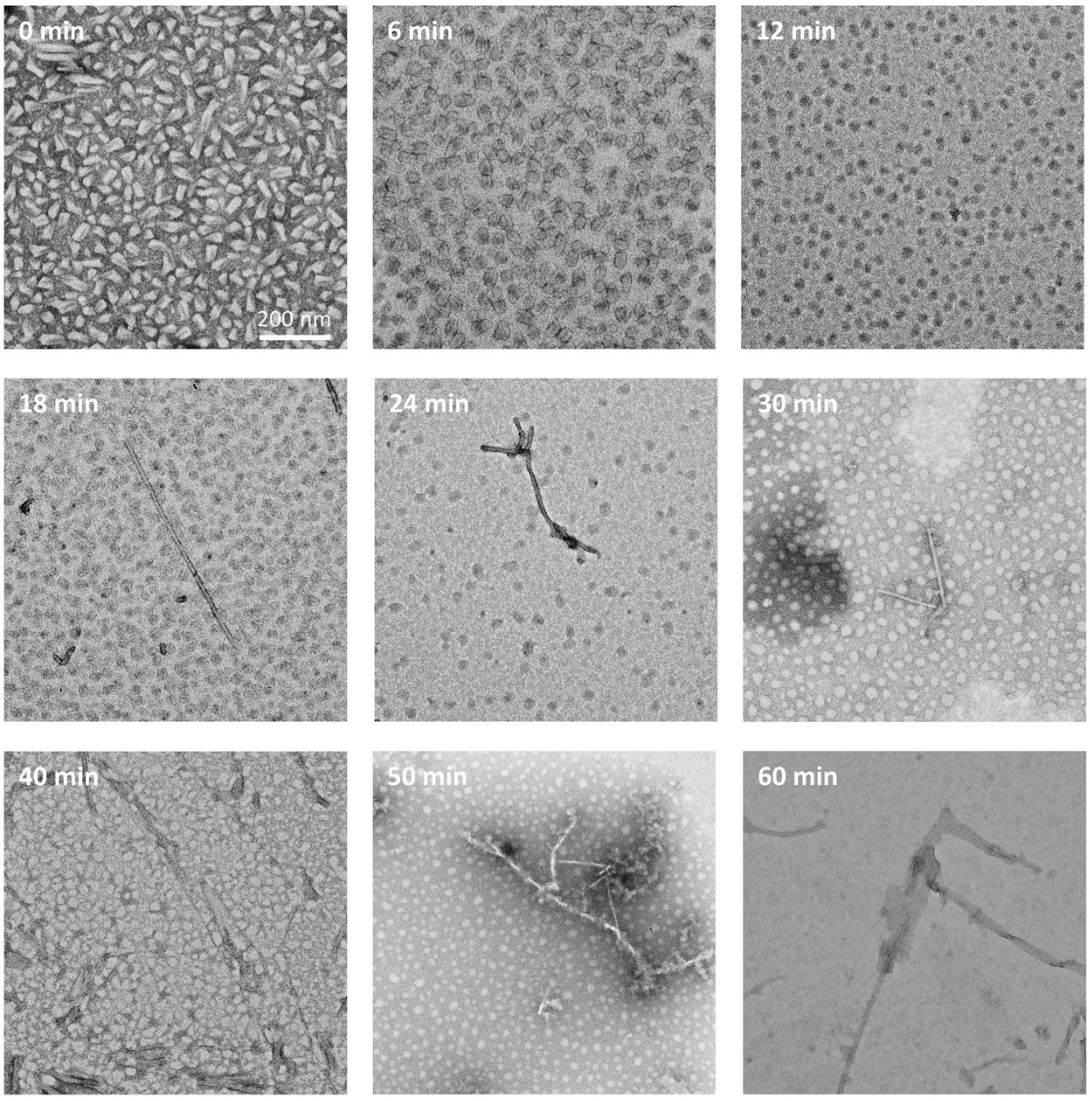

Figure S2. TEM images of LAFH (40 μM in water, V_{DMSO}:V_{water} = 1:99) without Ca^{2+} at 0, 6, 12, 18, 24, 30, 40, 50 and 60 min.

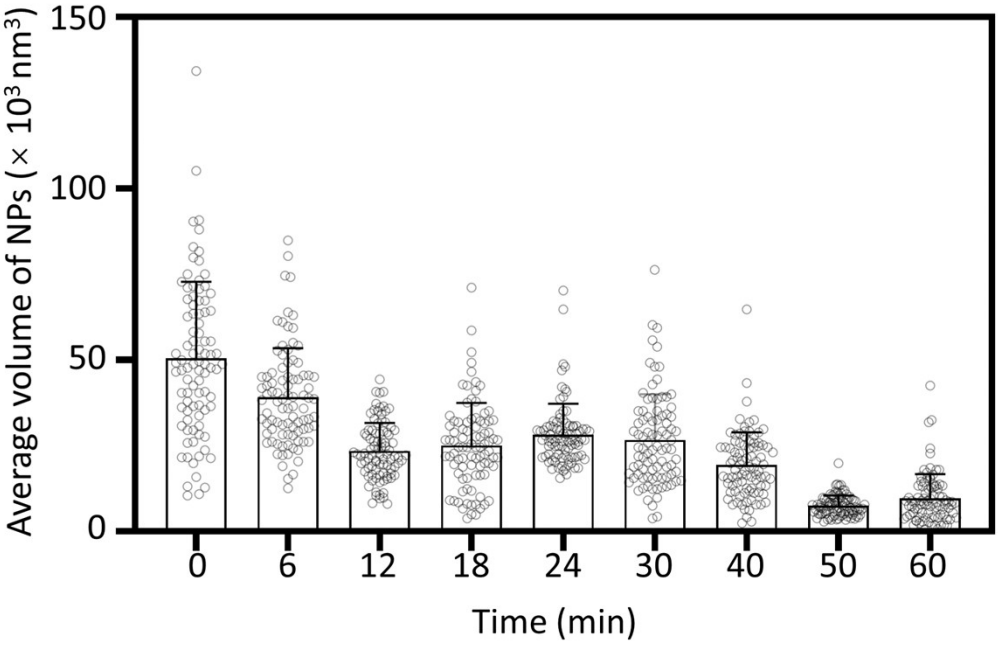

Figure S3. Average volume of NPs of LAFH (40 μM in water, V_{DMSO}:V_{water} = 1:99) without Ca^{2+} calculated through the length and width of NPs from TEM images. The quantitatively volumes were average of 50 NPs in 5 different TEM images.

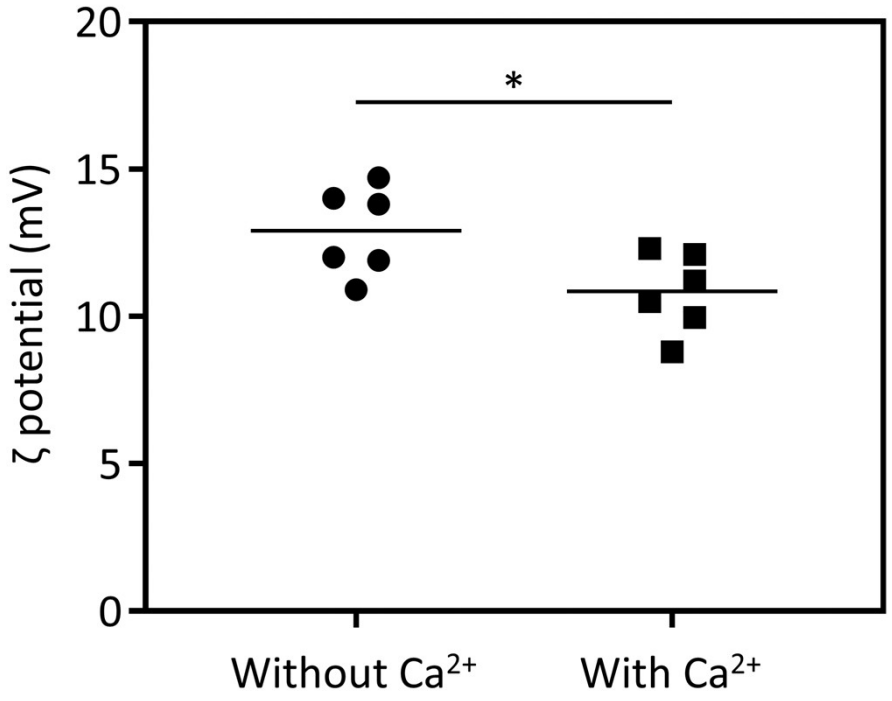

Figure S4. ζ potential of LAFH NPs (40 μM in water, V_{DMSO}:V_{water} = 1:99) with or without Ca^{2+} (40 μM) at 0 min. The significance analysis was calculated by Student's t-test. *P < 0.05.

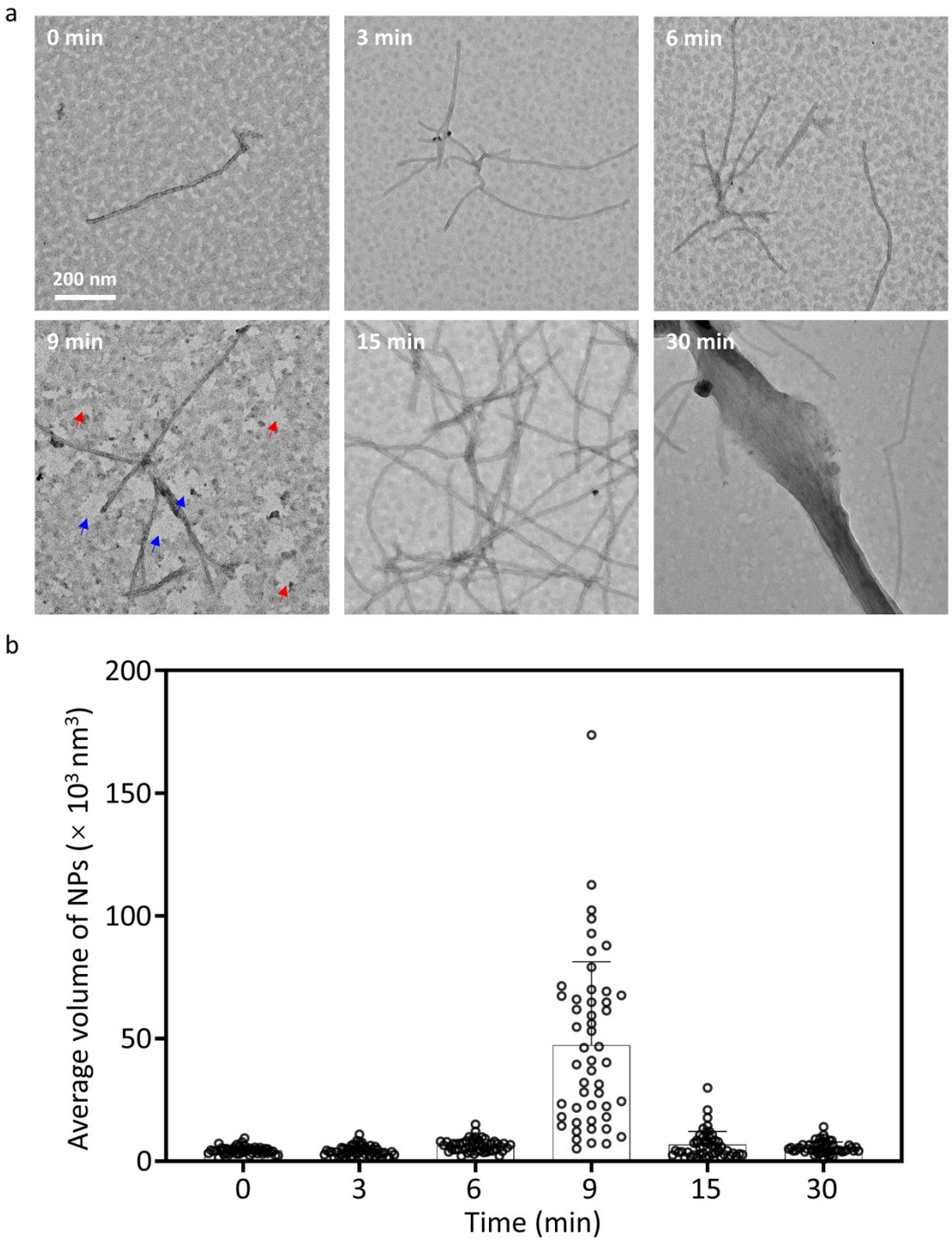

Figure S5. a) TEM images of LAFH (40 μM in water, V_{DMSO}:V_{water} = 1:99) incubated with Ca^{2+} (400 μM) at 0, 3, 6, 9, 15, 30 min. Blue arrows for NPs binding with fibril and red arrows for unbinding NPs. b) Average volume of NPs calculated through the length and width of NPs from TEM images. The quantitatively volumes of NPs were average of 50 NPs in 5 different TEM images.

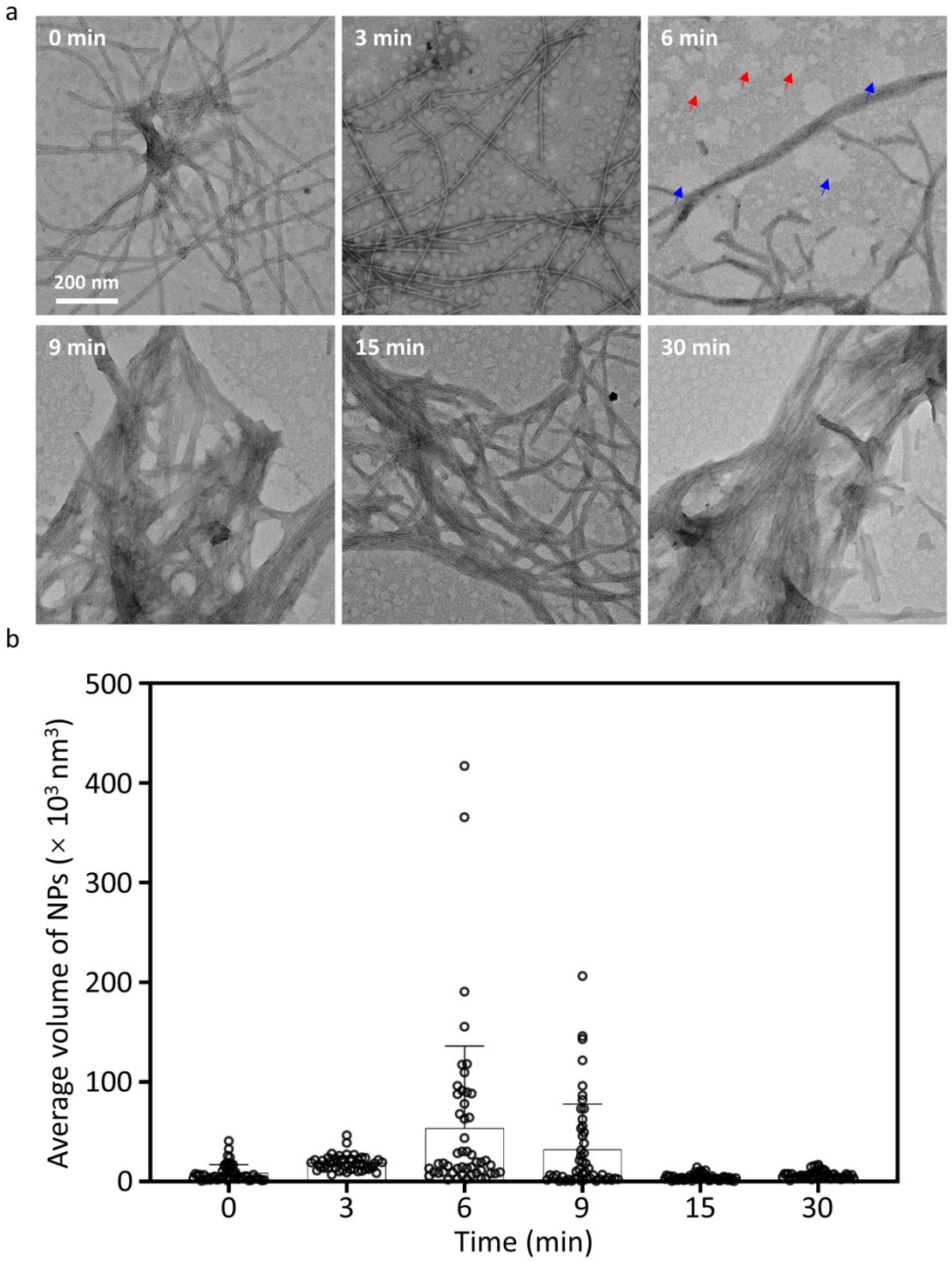

Figure S6. a) TEM images of LAFH (40 μM in water, V_{DMSO}:V_{water} = 1:99) incubated with Ca^{2+} (4000 μM) at 0, 3, 6, 9, 15, 30 min. Blue arrows for NPs binding with fibril and red arrows for unbinding NPs. b) Average volume of NPs calculated through the length and width of NPs from TEM images in (a). The quantitatively volumes of NPs were average of 50 NPs in 5 different TEM images.

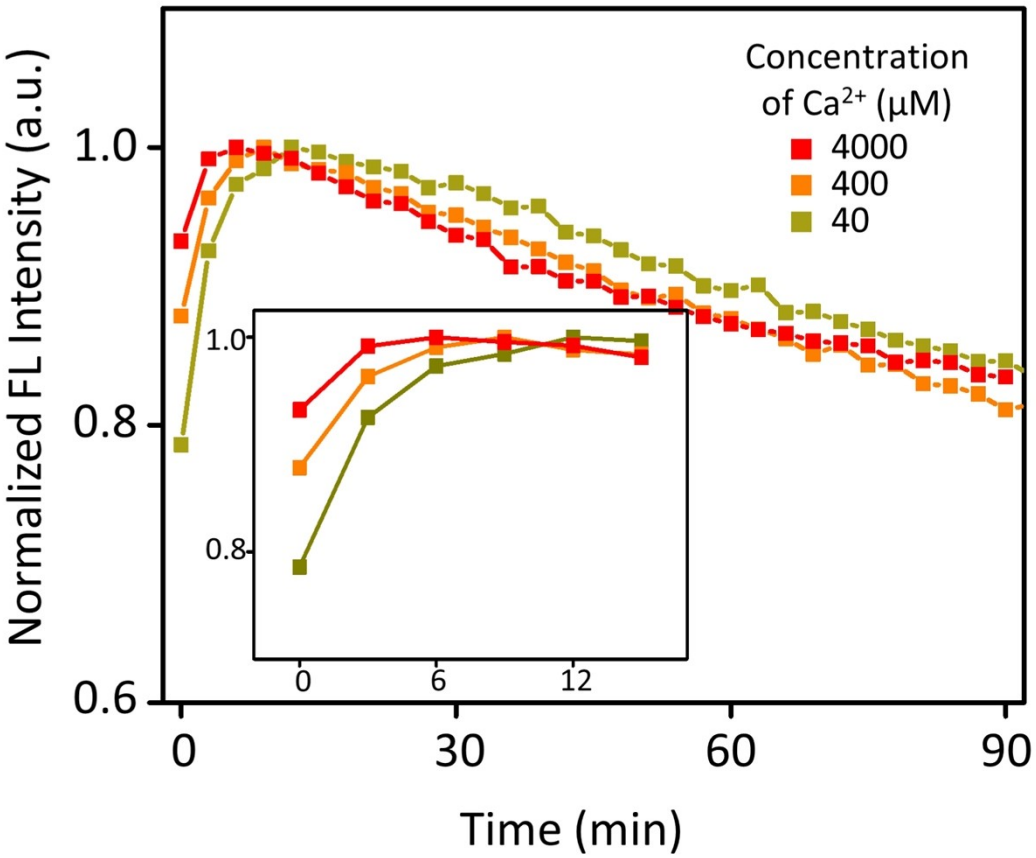

Figure S7. Normalized fluorescence intensity of ANS to LAFH (40 μM in water, V_{DMSO}:V_{water} = 1:99) in the absence or presence of Ca^{2+} (40, 400 or 4000 μM) in the first 90 min. The peak of ANS fluorescence intensity for 40, 400, 4000 μM was at 12, 9, 6 min, respectively. Each point was the average of 6 data.

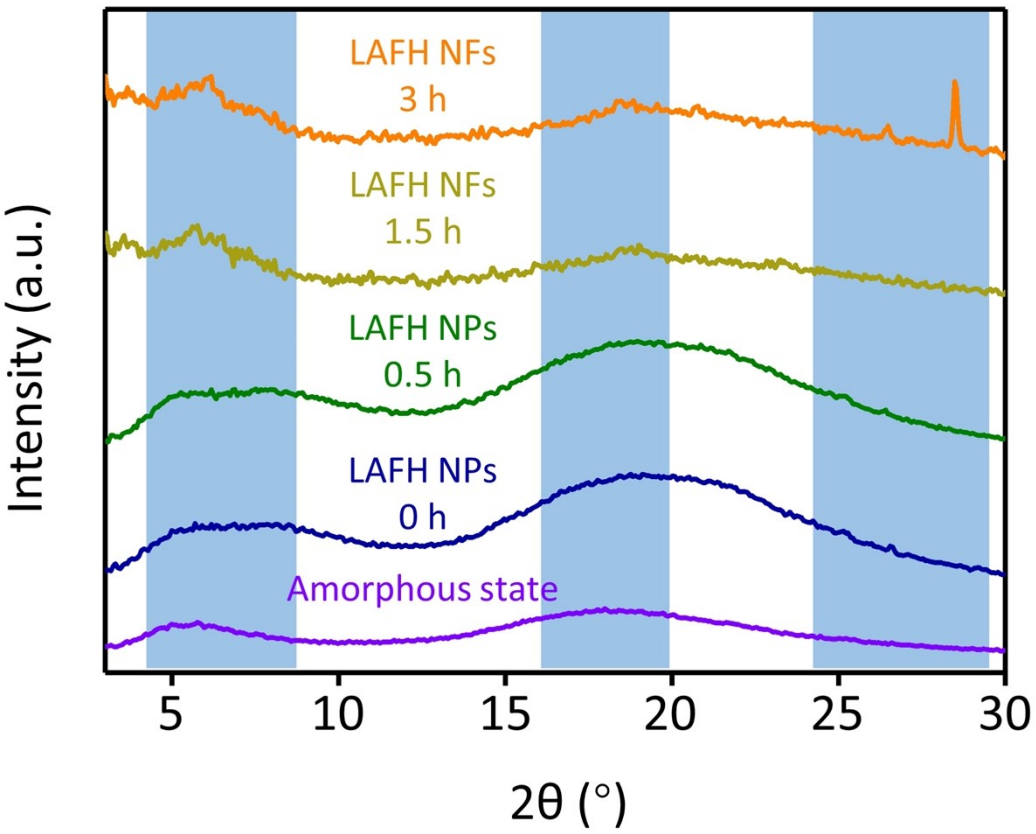

Figure S8. Powder XRD spectra of LAFH amorphous state as well as lyophilized LAFH (40 μM in water, V_{DMSO}:V_{water} = 1:99) incubated with Ca^{2+} (40 μM) after 0, 0.5, 1.5 and 3 h.

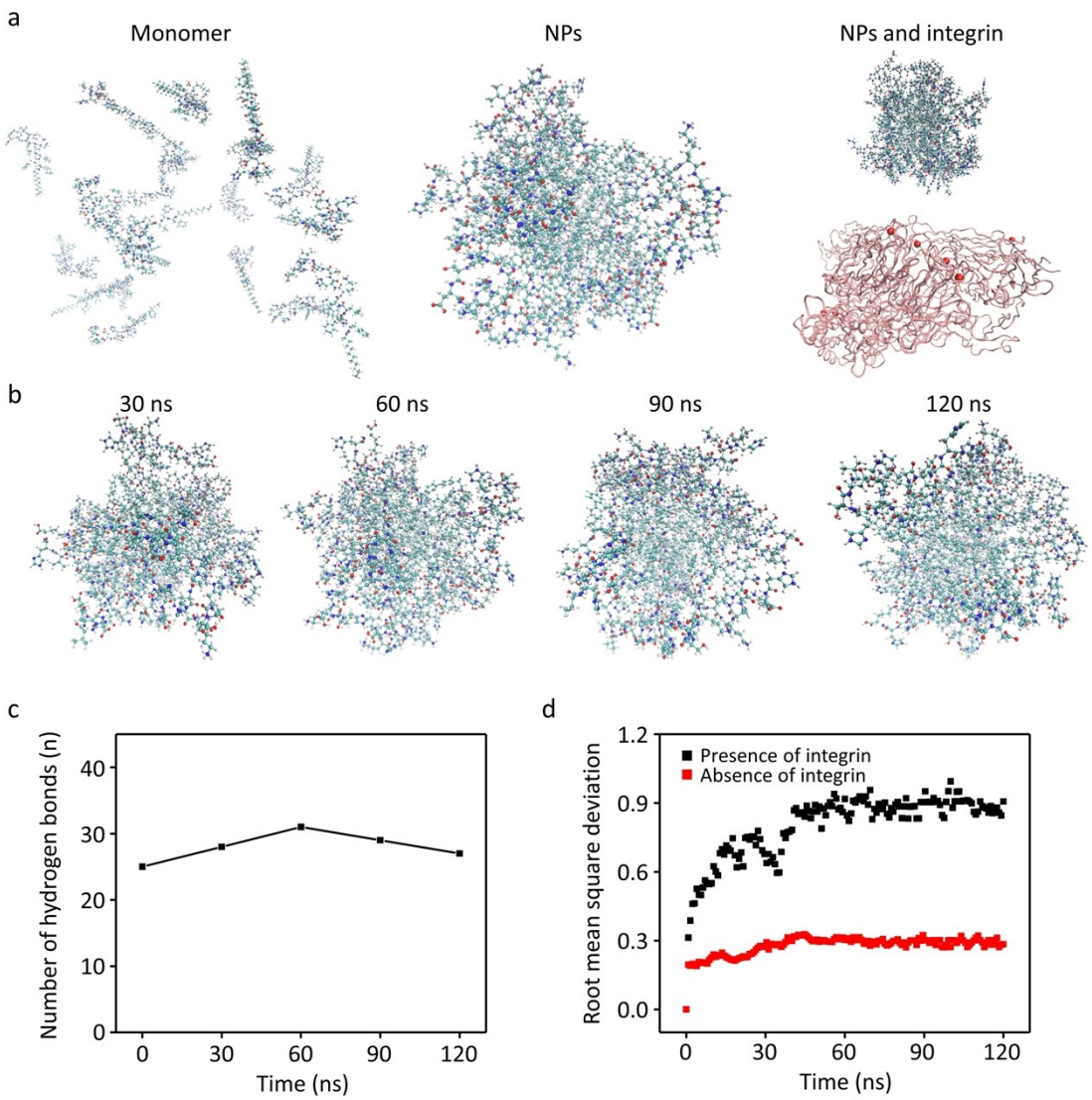

Figure S9. Molecular dynamics simulation on the fibrillogenesis of LAFH in the absence of integrin $\alpha_v\beta_3$. a) Snapshots on the 20 LAFH monomers, self-assembled NPs, and the culture between NPs and one integrin. Red ribbons for integrin $\alpha_v\beta_3$ and red balls for Ca^{2+}. b) Snapshots on the fibrillogenesis of LAFH NPs from (a) in the absence of integrin $\alpha_v\beta_3$ at different time point. c) Quantitatively analysis on the number of hydrogen bonds during the fibrillogenesis of LAFH in the absence of integrin $\alpha_v\beta_3$. d) Quantitatively analysis on the root mean square deviation during the fibrillogenesis of LAFH in the presence or in the absence of integrin $\alpha_v\beta_3$.

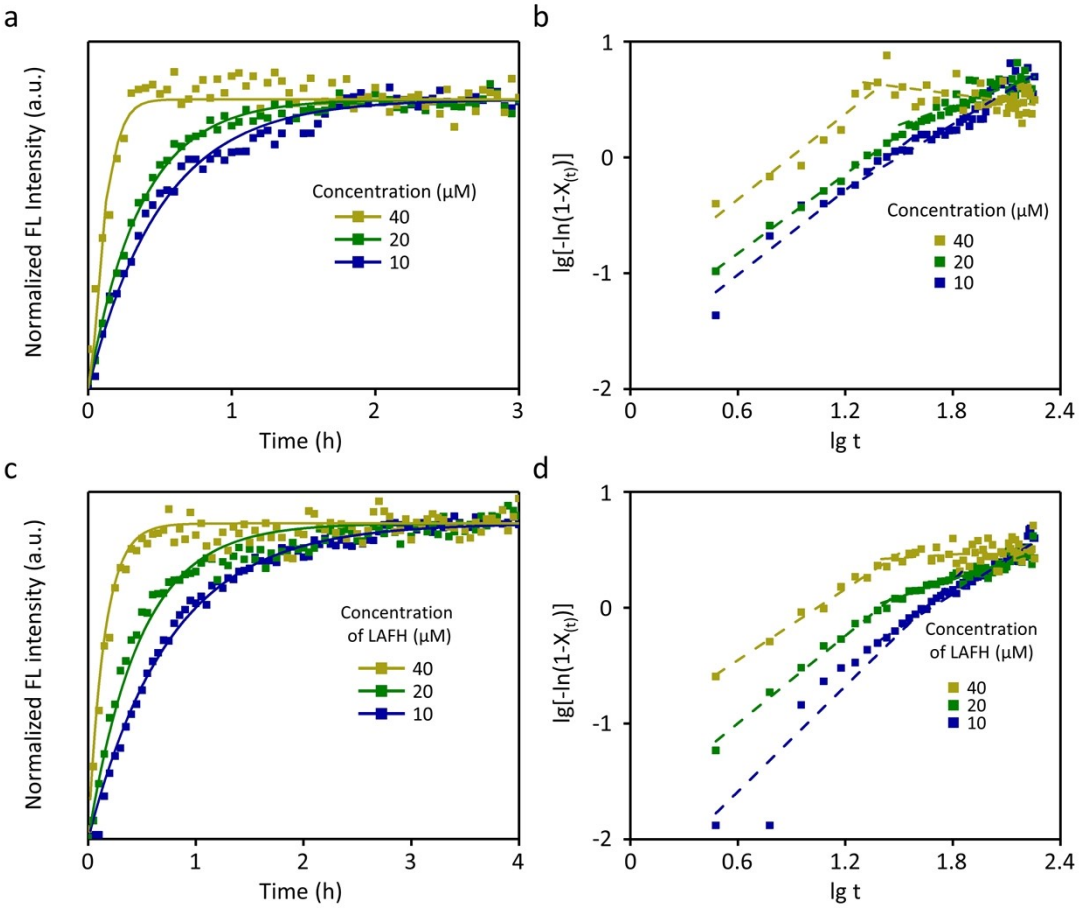

Figure S10. ThT fluorescence of LAFH. a) Normalized ThT fluorescence in LAFH of different concentration (10, 20 and 40 μM) in the absence of Ca^{2+}. Dots for fluorescence intensity of ThT and lines for fitted curve. b) Avrami curve for LAFH (10, 20 and 40 μM) in the absence of Ca^{2+} calculated from (a). c) Normalized ThT fluorescence in LAFH of different concentration (10, 20 and 40 μM) with Ca^{2+} (40 μM). Dots for fluorescence intensity of ThT and lines for fitted curve. d) Avrami curve for LAFH (10, 20 and 40 μM) with Ca^{2+} (40 μM) calculated from (c).

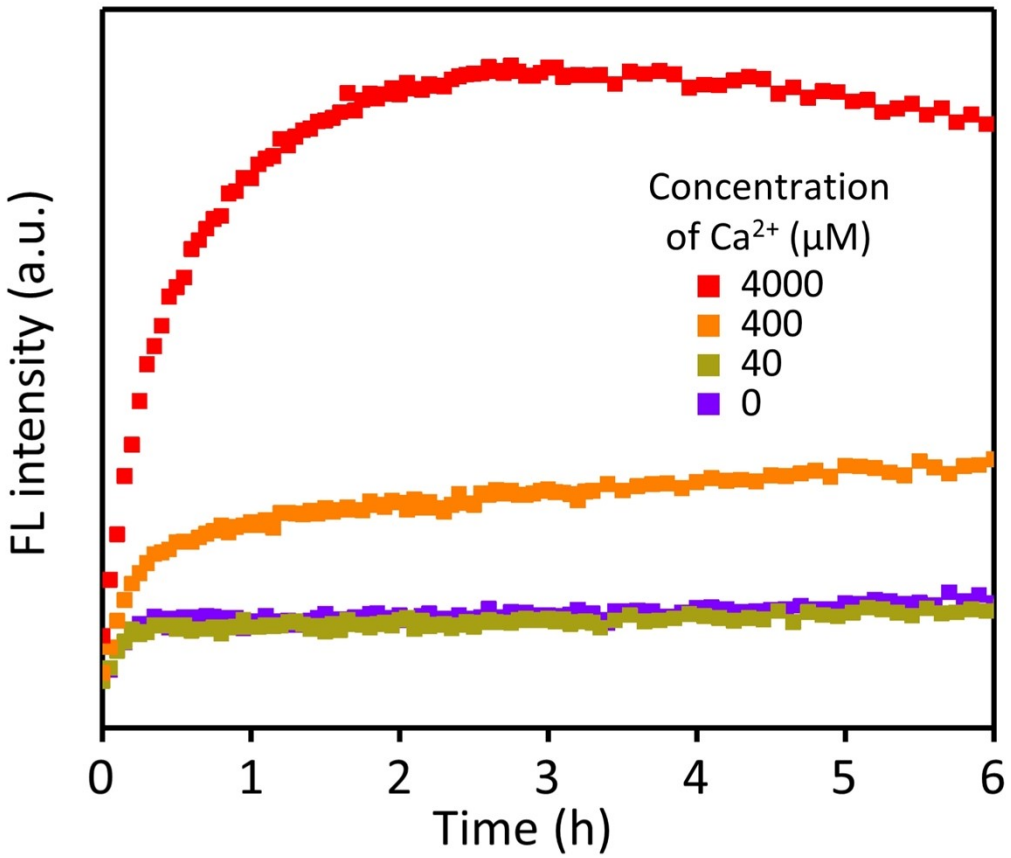

Figure S11. The kinetic of LAFH (40 μM in water, V_{DMSO}:V_{water} = 1:99) with different concentration of Ca^{2+} (0, 40, 400 or 4000 μM), suggesting higher concentration of Ca^{2+} could achieve higher level of fibrillogenesis. Each point was the average of 6 data.

References

1. G. Meisl, J. B. Kirkegaard, P. Arosio, T. C. T. Michaels, M. Vendruscolo, C. M. Dobson, S. Linse and T. P. J. Knowles, *Nat. Protoc.*, 2016, **11**, 252-272.
2. Y. Xu, S. Shang, J. Huang and S. Wan, *J. Mater. Sci.*, 2011, **46**, 4085-4091.